Neurobiology of Disease

PrP^C Homodimerization Stimulates the Production of PrP^C Cleaved Fragments PrPN1 and PrPC1

Maxime Béland, Julie Motard, Alice Barbarin, and Xavier Roucou
Department of Biochemistry, Faculty of Medicine, University of Sherbrooke, Sherbrooke, Quebec J1E 4K8, Canada

An endoproteolytic cleavage termed α-cleavage between residues 111/112 is a characteristic feature of the cellular prion protein (PrP^C). This cleavage generates a soluble N-terminal fragment (PrPN1) and a glycosylphosphatidylinositol-anchored C-terminal fragment (PrPC1). Independent studies demonstrate that modulating PrP^C α-cleavage represents a potential therapeutic strategy in prion diseases. The regulation of PrP^C α-cleavage is unclear. The only known domain that is essential for the α-cleavage to occur is a hydrophobic domain (HD). Importantly, the HD is also essential for the formation of PrP^C homodimers. To explore the role of PrP^C homodimerization on the α-cleavage, we used a well described inducible dimerization strategy whereby a chimeric PrP^C composed of a modified FK506-binding protein (Fv) fused with PrP^C and termed Fv-PrP is incubated in the presence of a dimerizer AP20187 ligand. We show that homodimerization leads to a considerable increase of PrP^C α-cleavage in cultured cells and release of PrPN1 and PrPC1. Interestingly, enforced homodimerization increased PrP^C levels at the plasma membrane, and preventing PrP^C trafficking to the cell surface inhibited dimerization-induced α-cleavage. These observations were confirmed in primary hippocampal neurons from transgenic mice expressing Fv-PrP. The proteases responsible for the α-cleavage are still elusive, and in contrast to initial studies we confirm more recent investigations that neither ADAM10 nor ADAM17 are involved. Importantly, PrPN1 produced after PrP^C homodimerization protects against toxic amyloid-β (Aβ) oligomers. Thus, our results show that PrP^C homodimerization is an important regulator of PrP^C α-cleavage and may represent a potential therapeutic avenue against Aβ toxicity in Alzheimer's disease.

Introduction

Prion diseases or transmissible spongiform encephalopathies (TSEs) are fatal neurodegenerative disorders. TSEs result from the conversion of the cellular isoform of the prion protein (PrP^C) into its β-sheet-rich pathological counterpart PrP^{Sc} (Prusiner et al., 1998). PrP^C is a glycosylphosphatidylinositol (GPI)-anchored protein mainly present at the plasma membrane. Its role in the pathology is well established since PrP^C expression is necessary for the development of TSEs (Büeler et al., 1993; Brandner et al., 1996; Mallucci et al., 2003). In contrast, its physiological function is still under debate (Roucou et al., 2004; Steele et al., 2007). PrP^C undergoes several physiological cleavages, the β- and α-cleavage, at amino acids 89/90 and 110–111/112 of human PrP^C, respectively; and a cleavage at amino acids 228/229 resulting in ectodomain shedding (Chen et al., 1995; Mangé et al., 2004; Taylor et al., 2009).

The α-cleavage (also termed C1 cleavage) produces a 17 kDa, N-terminally truncated fragment termed PrPC1, anchored to the plasma membrane and a secreted 11 kDa fragment termed PrPN1 (Chen et al., 1995; Mangé et al., 2004). Opposite functions were attributed to PrPC1 (Sunyach et al., 2007; Lewis et al., 2009; Westergard et al., 2011). Overexpression of PrPC1 resulted in increased expression of p53 in HEK293 cells and potentiated staurosporine-induced apoptosis in HEK293 and primary neuronal cells (Sunyach et al., 2007). Yet PrPC1 is not neurotoxic in transgenic mice expressing PrPC1 (Westergard et al., 2011). In addition, PrPC1 is associated with protection against infection with the prion strain M1000 in cultured cells (Lewis et al., 2009). Finally, PrPC1 is not a substrate for conversion to PrP^{Sc} and acts as a dominant-negative inhibitor of this conversion *in vivo* (Westergard et al., 2011). PrPN1 also displays neuroprotective activity against *in vivo* ischemic stress and against oligomeric amyloid-β (Aβ)-associated cell death in primary neurons (Guillot-Sestier et al., 2009, 2012; Resenberger et al., 2011). Overall, these studies point to a possible neuroprotective activity associated with α-cleavage of PrP^C. In favor of this hypothesis, PrP^{Sc} and toxic PrP mutants are impaired in their α-cleavage (Oliveira-Martins et al., 2010).

The mechanism by which the α-cleavage is regulated is still poorly defined. Yet the regulation of and finding the endoproteolytic protease responsible for PrP^C α-cleavage (α-PrPase) may be relevant therapeutic strategies for treatment of TSEs (Oliveira-Martins et al., 2010; Resenberger et al., 2011). There is evidence that the metalloproteases ADAM10 (a disintegrin and metalloproteinase) and ADAM17 are responsible for the constitutive and

Received May 8, 2012; revised July 17, 2012; accepted Aug. 8, 2012.

Author contributions: X.R. designed research; M.B., J.M., and A.B. performed research; M.B., J.M., and X.R. contributed unpublished reagents/analytic tools; M.B., J.M., and X.R. analyzed data; M.B. and X.R. wrote the paper.

This work was supported by Canadian Institutes for Health Research Grant MOP-89881 (X.R.). M.B. was supported by a scholarship from the Fonds de la Recherche en Santé du Québec. The anti-ADAM17 was kindly provided by Dr. Claire M. Dubois (University of Sherbrooke, Sherbrooke, QC, Canada). CHO-7PA2 cells were a kind gift from Drs. Dennis J. Selkoe (Harvard University, Cambridge, MA) and Marco Antonio Maximo Prado (University of Western Ontario, London, ON, Canada).

The authors declare no competing financial interests.

Correspondence should be addressed to Dr. Xavier Roucou, Department of Biochemistry (Z8-2001), Faculty of Medicine, University of Sherbrooke, 3201 Jean Migneault, Sherbrooke, Quebec J1E 4K8, Canada. E-mail: xavier.roucou@usherbrooke.ca.

DOI:10.1523/JNEUROSCI.2236-12.2012

 0270-6474/12/3213255-09$15.00/0

PKC-regulated α-cleavage in cultured cells, respectively, and high levels of PrPC1 in the human brain correlates with the presence of active ADAM10 (Vincent et al., 2001; Laffont-Proust et al., 2005; Liang et al., 2012). However, α-cleavage occurs normally in neuron-specific ADAM10 knock-out mice and the search for other proteases that have the ability to perform the α-cleavage continues (Altmeppen et al., 2011). The hydrophobic domain (HD) (amino acids 111–129) of PrP^C is essential for the α-cleavage both *in cellulo* and *in vivo* (Bremer et al., 2010; Oliveira-Martins et al., 2010). Interestingly, the HD is also essential for PrP^C homodimerization and the stress-protective activity of PrP^C (Rambold et al., 2008).

Together, these results led us to speculate that the homodimerization of PrP^C could regulate its α-cleavage. Since α-cleavage occurs intracellularly in a late compartment of the secretory pathway (Walmsley et al., 2009), we used a dimerization strategy based on a permeable homodimerizer AP20187 and one FK506 binding domain (Fv) fused to PrP^C (Spencer et al., 1993; Goggin et al., 2007). Here, we show that enforced homodimerization considerably increases the release of PrPN1 and PrPC1 in cultured cells and in primary neurons due to an increase of PrP^C trafficking. We also show that PrPN1 secreted after PrP^C homodimerization has protective functions against Aβ-associated cell death.

Materials and Methods

Antibodies. Primary antibodies used were rabbit monoclonal anti-prion EP1802Y (Abcam), mouse anti-influenza hemagglutinin epitope (HA) (Covance; clone HA.11), mouse monoclonal anti-Aβ (Covance; clone 6E10), mouse monoclonal anti-prion SAF32 (Cayman Chemical), rabbit polyclonal anti-phosphorylated p44/p42 MAPK, rabbit polyclonal anti-ERK1 (Cell Signaling Technology; clone C-16), mouse monoclonal anti-β-actin (Sigma-Aldrich; clone ac-15), and mouse monoclonal anti-N-cadherin (BD Biosciences). Rabbit polyclonal anti-ADAM17/TACE was kindly provided by Dr. Claire M. Dubois (University of Sherbrooke, Sherbrooke, QC, Canada). Secondary antibodies used were donkey anti-rabbit and anti-mouse HRP-conjugated antibodies (GE Healthcare).

Constructs, transfection, stable cell lines, and dimerization. PrP^C, Fv-PrP, and Fv-PrPΔGPI cDNAs were described previously (Goggin et al., 2007). Human embryonic kidney (HEK) cells were cultured in DMEM supplemented with 10% fetal bovine serum. Cells were maintained at 37°C in 5% CO_2 in air. Stable expression of Fv-PrP and Fv-PrPΔGPI in HEK cells were obtained from transfection performed using GeneCellin (BioCellChallenge) according to the manufacturer's protocol. The stable cell lines were selected and kept in the culture medium supplemented with 125 μg/ml hygromycin (Wisent). For homodimerization of Fv-PrP, stable cells were plated and incubated for 36 h. The culture medium was replaced with fresh medium supplemented with vehicle (−AP) or 200 nM of the dimerizer AP20187 (+AP) for 4 or 20 h (where indicated) at 37°C and in a 5% CO_2 atmosphere. AP20187 was purchased from Invitrogen.

Immunoprecipitation, Western blot, and PNGase F treatment. For PrPN1 immunoprecipitation, 1 ml of supernatant from cells grown in six-well plates and treated with vehicle or with the dimerizer AP20187 was collected and subjected to immunoprecipitation with an anti-HA affinity matrix (Fv-PrP-expressing cells) or SAF32 anti-PrP antibodies (PrP-expressing cells) for 4 h according to the manufacturer's protocol (Roche Applied Science). The matrix was washed three times using PBS, and bound proteins were eluted by incubating for 3 min at 95°C in 4× SDS-PAGE sample buffer [0.5% SDS (w/v), 1.25% 2-mercaptoethanol (v/v), 4% glycerol (v/v), 0.01% bromophenol blue (w/v), 15 mM Tris-HCl, pH 6.8]. After electrophoresis, proteins were transferred on PVDF membrane according to manufacturer's protocol and immunodetected using appropriate antibodies.

Cells were lysed in 27 μM ammonium hydroxide (NH_4OH) (Bioshop) for 5 min and sonicated. Samples were quantified using BCA protein assay reagent (Thermo Fisher Scientific), and 200 μg of protein from each sample was precipitated using the chloroform/methanol technique described by Wessel and Flügge (1984). Proteins samples were resuspended in 4× SDS-PAGE sample buffer and boiled for 3 min before electrophoresis and Western blot analysis.

Deglycosylation of cells lysates with PNGase F (New England Biolabs) was performed according to the manufacturer's protocol. Briefly, 20 μg of protein extracted in NH_4OH was supplemented with NP-40, boiled for 10 min, and digested with 500 U of PNGase F for 60 min at 37°C. Samples were resuspended in 4× SDS-PAGE sample buffer before electrophoresis and Western blot analysis.

MAP kinases p44^{ERK1} and p42^{ERK2} phosphorylation. Fv-PrP-expressing cells were treated with vehicle, with the dimerizer AP20187, or with PrP^C antibody SAF32 for 5 and 30 min. Cells were lysed with NH_4OH supplemented with 1× phosphatase inhibitor (Thermo Fisher Scientific) and sonicated. Cell lysates were quantified using BCA protein assay reagent and subjected to SDS-PAGE and Western blot analysis. Phosphorylation of MAP kinases p44^{ERK1} and p42^{ERK2} was normalized to total ERK expression levels by densitometry.

Reactive oxygen species detection. The oxidable probe 2′,7′-dichlorofluorescein (DCF-DA) (Calbiochem) was added directly to the medium at a concentration of 10 μM, and then incubated at 37°C for 30 min. Cells were treated with vehicle or with the dimerizer AP20187 for 30 min at 37°C. Cells were examined with a scanning confocal microscope (FV1000; Olympus) coupled to an inverted microscope with a 63× oil-immersion objective (Olympus). Cells were laser excited at 488 nm (40 mW argon laser). Serial horizontal optical sections of 1600 × 1600 pixels with two times line averaging were taken. Images were acquired during the same day, typically from three randomly selected fields from each experimental condition using identical settings of the instrument.

ADAMs mRNA expression and RT-PCR. Human monocytes U-937 were cultured in RPMI 1640 with 10% fetal bovine serum. Total cellular RNA was extracted from U-937 and HEK cells expressing Fv-PrP using Qiazol according to the manufacturer's protocol (QIAGEN). Five micrograms of total RNA extract were treated with the RQ1 DNase (Promega). Complementary DNA was synthesized from 2.5 μg of total RNA with the AMV reverse transcriptase (New England Biolabs) using oligo-dT 15 primers (Promega). In control experiments, the reverse transcription mixture lacked the AMV reverse transcriptase. PCR amplification was performed using the Phusion High-Fidelity DNA polymerase (New England Biolabs) and specific primers as follows: for ADAM8 (909 bp), forward, 5′-gtcctgcttctcctatgacatcctac-3′, and reverse, 5′-ttttt-gtggatccgggtgctgtgggagctccggc-3′; ADAM10 (243 bp), forward, 5′-gctgaatggattgtggctcattggtg-3′, and reverse, 5′-ctgcagttagcgtctcatgtgtcc-3′; ADAM17 (309 bp), 5′-agcagcatggattctgcatcgg-3′; and ADAM17R2, 5′-gctgtcaacacgattctgacgct-3′.

ADAMs inhibition. Vehicle or the general metalloprotease inhibitor marimastat (Calbiochem) was added directly to the medium at a concentration of 10 μM. After 30 min, cells were treated with vehicle or the dimerizer AP20187 in the presence of 10 μM marimastat. Supernatants and cell lysates were collected after 24 h. PrPN1 was recovered from supernatants by immunoprecipitation. Immunoprecipitates and cell lysates were subjected to SDS-PAGE and Western blot analysis.

ADAM10 and ADAM17 inhibition. Inhibition of ADAM10 and ADAM17 through siRNA gene silencing was performed as described previously (Kwak et al., 2009). Briefly, cells were transfected twice with the SMARTpool siRNA against ADAM10 or ADAM17/TACE (Dharmacon RNAi Technology) or the off-target siRNA lamin A/C (Dharmacon RNAi Technology) using GeneCellin according to the manufacturer's protocol. Supernatant and cell lysates were collected and subjected to Western blot analysis.

Quantification of plasma membrane Fv-PrP postdimerization. Homodimerization of Fv-PrP was induced for 4 h. Cells in 24-well plates were washed with PBS and treated with 0.2 ml of Opti-MEM containing 0.2 U of phosphatidylinositol-specific phospholipase C (PI-PLC) (Invitrogen) for 2 h at 37°C and in a 5% CO_2 atmosphere. A volume of 0.02 ml of the conditioned medium was subjected to PNGase F treatment. PI-PLC-treated cells were lysed with NH_4OH. Lysates were subjected to Western blot analysis with anti-β-actin antibodies to confirm that similar amounts of cells were used.

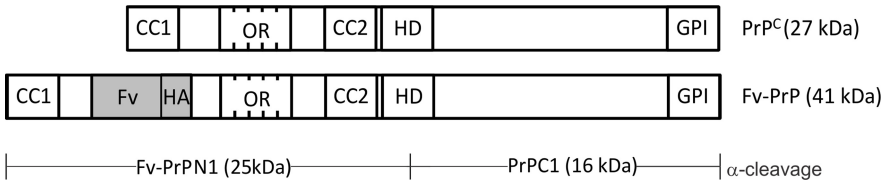

Figure 1. Schematic representation of PrP^C and Fv-PrP. The charge cluster 1 (CC1), the octapeptide repeat (OR), the charge cluster 2 (CC2), and the hydrophobic domain (HD) are depicted on both PrP^C and Fv-PrP. The inducible dimerization domain (Fv) containing a HA tag is inserted between the CC1 and the OR (Goggin et al., 2007). The α-cleavage is represented with the associated proteolytic fragments length.

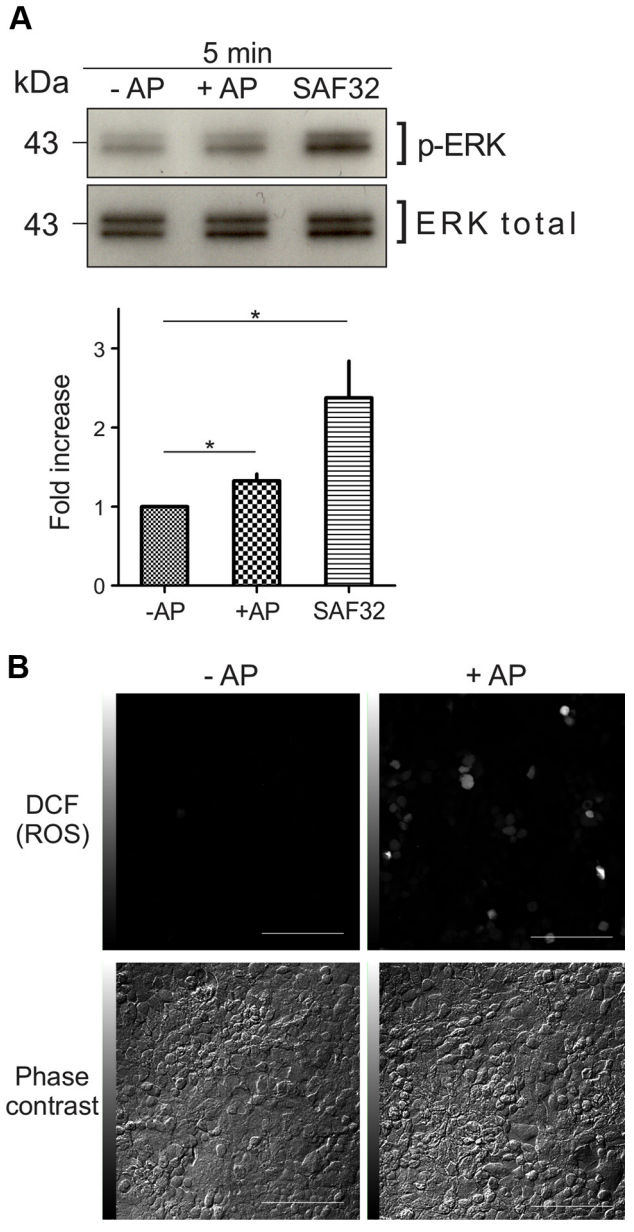

Figure 2. Dimerization of PrP^C induces the phosphorylation of the MAP kinase p44^{ERK1}, p42^{ERK2}, and ROS production. ***A***, Western blot analysis of ERK using anti-phospho and anti-total p44^{ERK1} and p42^{ERK2} antibodies. Fv-PrP-expressing cells were treated with vehicle (−AP), AP20187 (+AP), or the anti-PrP^C SAF32 for 5 min Western blots are representative of four independent experiments. A densitometric analysis is shown (*$p < 0.05$). Error bars indicate SEM. ***B***, Fv-PrP-expressing cells were loaded with 2′,7′-dichlorofluorescein diacetate (DCF) before the addition of vehicle (−AP) or AP20187 (+AP). ROS production was visualized by confocal microscopy 30 min after dimerization. Scale bar, 100 μm. Images for ROS detection are representative of three independent experiments.

Animals. Murine Fv-PrP was amplified (forward primer, 5′-TAC TCG AGC CGC CAT GGC GAA CCT TGG CTA CTG G-3′, and reverse primer, 5′-TAC TCG AGT CAT CCC ACG ATC AGG AAG ATG AGG-3′) and cloned into the XhoI site of MoPrP.Xho (Borchelt et al., 1996). The targeting DNA was excised with NotI restrictive enzyme and microinjected into the pronucleus of fertilized C57BL/6 mice. Founder lines were identified by PCR for the transgene using the forward primer (5′-CTA CTG GCT GCT GGC CCT CTT TGT GA-3′) and the reverse primer (5′-TGT GGA CTG ATG TCG GCC TCT GC-3′). Founders were bred to wild-type C57BL/6 mice. All experiments requiring animals were performed in accordance with a protocol reviewed and approved by the Institutional Animal Research Review Committee of the University of Sherbrooke (approval ID number 233-10) in conformity with the Canadian Council on Animal Care.

Dimerization of Fv-PrP in primary neurons. Primary hippocampal and cortical culture was performed as described by Lopes et al. (2005). Briefly, primary neuronal cultures were obtained from E15 brains of homozygote (*Fv-PrP*$^{+/+}$) transgenic mice expressing murine Fv-PrP. The hippocampal structure or the cortex was aseptically dissected in HBSS (Invitrogen) and treated with trypsin (0.06%) in HBSS for 20 min at 37°C. The protease was inactivated with 10% FCS in Neurobasal medium (Invitrogen) for 5 min. After three washes with HBSS, cells were mechanically dissociated in Neurobasal medium containing B-27 supplement (Invitrogen), glutamine (2 mM; (Invitrogen), penicillin (100 U), and streptomycin (100 μg/ml). The cells (1×10^6 cells) were plated onto poly-L-lysine-precoated plates for 36 h at 37°C and in a 5% CO_2 atmosphere. After induction of homodimerization of Fv-PrP, supernatant and cells lysates were collected.

Neuroprotection assays. Neuroprotection assays were performed as previously described (Resenberger et al., 2011). CHO-7PA2 cells were a kind gift from Drs. Dennis J. Selkoe (Harvard University, Cambridge, MA) and Marco Antonio Maximo Prado (University of Western Ontario, London, ON, Canada). CHO-7PA2 cells were cultured in DMEM supplemented with 10% fetal bovine serum and 200 μg/ml geneticin (G418). Cells were maintained at 37°C in 5% CO_2 in air. Conditioned medium of CHO-7PA2 cells were mixed with conditioned medium from homodimerized Fv-PrP-expressing cells in a 1:1 ratio and added to 50% confluent CHO-7PA2 cells. Coverslips of seeded PrP^C-expressing cells were cocultured with the CHO-7PA2 for 48 h.

For active caspase-3 immunofluorescence, coverslips of Fv-PrP-expressing cells were fixed with 4% paraformaldehyde for 10 min, permeabilized in 0.15% Triton X-100 for 5 min, and blocked with 10% normal goat serum for 60 min in PBS. Cells were stained for 16 h with an anti-active caspase-3 antibody followed by incubation with a fluorescently conjugated secondary antibody (Invitrogen) for 60 min. Nuclei were stained with Hoechst and mounted onto glass slides.

Terminal deoxynucleotidyl transferase-mediated biotinylated UTP nick end labeling (TUNEL) assay was performed according to the manufacturer's protocol (Promega). Briefly, coverslips of Fv-PrP-expressing cells were fixed with 4% paraformaldehyde for 25 min at 4°C, permeabilized in 0.15% Triton X-100 for 5 min, and treated with the equilibration buffer for 10 min. Terminal deoxynucleotidyl transferase reaction was performed in the dark for 60 min at 37°C and stopped by immersion of the cells in 2× SSC. Nuclei were stained with Hoechst and mounted onto glass slides.

Active caspase-3 immunofluorescence and TUNEL assays were examined by epifluorescence microscopy using an Eclipse TE2000-E visible/epifluorescence inverted microscope (Nikon Corporation) equipped with bandpass filters for fluorescence of Hoechst (excitation, D340/40; emission, D420) and GFP (excitation, D450/40; emission, D500/50) (Nikon Corporation). Photomicrographs of 1344 × 1024 pixels were captured using 10 and 20× objectives and Orca cooled color digital camera (Hamamatsu Photonics). Images were processed using NIS Elements AR software (Nikon Corporation). Totals of 3000 and 30,000 cells

were counted per conditions for immunofluorescence and TUNEL assays, respectively. Within the same figure, pictures were taken with the same exposure time.

Preparation of Aβ monomeric and oligomeric species. Ten milliliters of conditioned CHO-7PA2 medium was cleared of cells (200 × *g*; 10 min; 4°C), and concentrated to 0.5 ml by centrifugation through a 3K Amicon Ultra 15 filter unit. After lyophilization, the pellet was solubilized with 100 μl of SDS-PAGE sample buffer, and 25 μl was analyzed by Western blot with 6E10 antibodies.

Densitometric analyses and statistical analysis. All densitometric analyses were performed using ImageJ software on a minimum of three independent experiments. All values are expressed as means ± SEM. Data of the phosphorylation of the MAP kinase p44^{ERK1} and p42^{ERK2}, and of the normalized TUNEL and activated caspase 3 assays were analyzed by a paired Student *t* test. Data of the TUNEL and activated caspase-3 were analyzed by a two-way ANOVA. All statistical analyses were performed using GraphPad Prism 5 software.

Results

Enforced PrP^C homodimerization

We used a well characterized inducible homodimerization system based on the dimerization domain Fv containing a HA tag and the dimerizer AP20187 (Fig. 1) (Spencer et al., 1993; Eggert et al., 2009). In contrast to cross-linking antibodies, AP20187 is permeable and is able to target intracellular Fv-PrP. This is an essential characteristic since α-cleavage occurs in the late secretory pathway (Walmsley et al., 2009). Fv was inserted in the unstructured N-terminal moiety of PrP^C between the charge cluster 1 (CC1) (amino acids 23–31) and the octapeptide region (amino acids 51–91) (Fig. 1). The resulting protein is termed Fv-PrP, and we previously showed that insertion of the Fv domain does not interfere with folding, trafficking, localization, and glycosylation of the protein (Goggin et al., 2007). To verify the functionality of this homodimerization system, we assessed the phosphorylation of the MAP kinases p44^{ERK1} and p42^{ERK2} and the production of reactive oxygen species (ROS), two already-characterized effects of antibody-mediated PrP^C homodimerization (Schneider et al., 2003; Rambold et al., 2008). Homodimerization of Fv-PrP was triggered by adding the synthetic dimerizer AP20187 to HEK293 cells stably expressing Fv-PrP. The phosphorylation of the MAP kinases p44^{ERK1} and p42^{ERK2} was determined using an anti-phospho-p44^{ERK1} and -p42^{ERK2} antibodies (Fig. 2*A*). In a control experiment, Fv-PrP was cross-linked with SAF32 antibodies. As expected, SAF32-mediated cross-linking led to a significant increase (2.3 ± 0.9) of the phosphorylation of p44^{ERK1} and p42^{ERK2} after 5 min of incubation (Schneider et al., 2003). Similarly, dimerization of PrP^C with the dimerizer AP20187 led to a rapid increase (1.4 ± 0.1) of the phosphorylation of both p44^{ERK1} and p42^{ERK2} (Fig. 2*A*). Although PrP^C cross-linking resulted in higher levels of p44^{ERK1} and p42^{ERK2} compared with AP20187-mediated PrP^C dimerization, the slight increase was consistently observed and statistically significant. Phosphorylation of p44^{ERK1} and p42^{ERK2} returned to basal levels 30 min following SAF32-mediated cross-linking or treatment with AP20187 (data not shown).

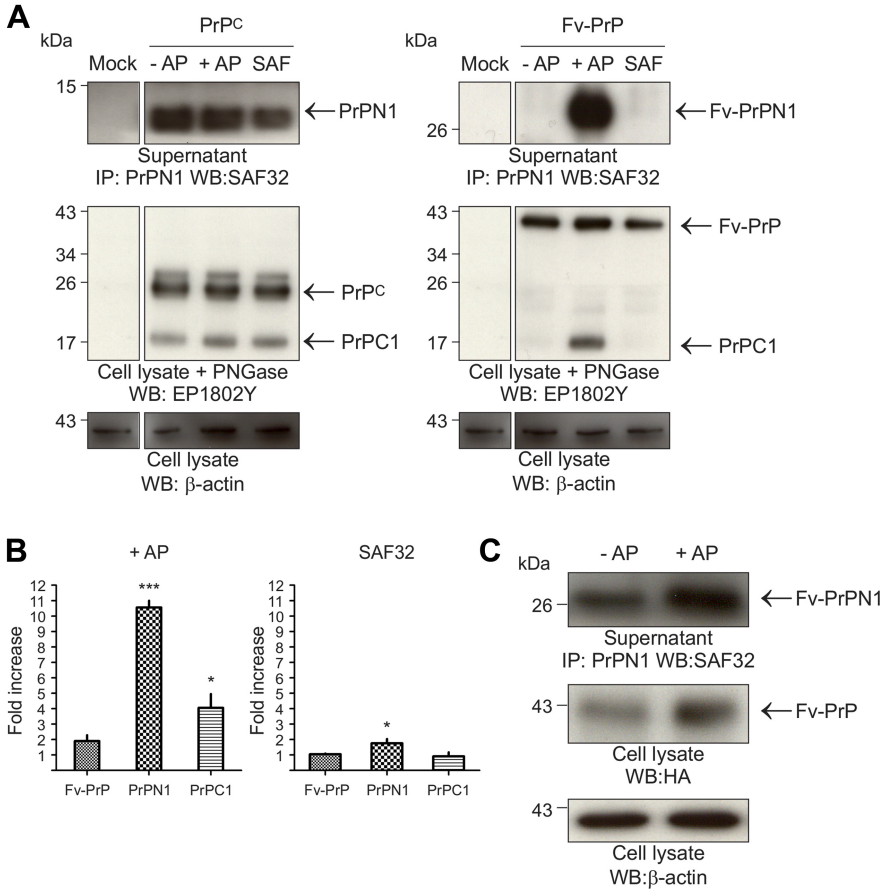

Figure 3. Dimerization of PrP^C induces a large increase of PrPN1 and PrPC1. ***A***, Western blot analysis of PrPN1, Fv-PrPN1, PrP^C, and PrPC1, and actin with SAF32, EP1802Y, and anti-actin antibodies. Mock-treated HEK293 cells, or PrP^C and Fv-PrP-expressing cells were treated with vehicle (−AP), AP20187 (+AP), or anti-PrP^C SAF32 antibodies for 20 h. PrPN1 was immunoprecipitated from the culture medium. Cell lysates were treated with PNGase to detect PrPC1. ***B***, Densitometric analysis of three independent experiments (*$p < 0.05$; ***$p < 0.0005$). Error bars indicate SEM. ***C***, Western blot analysis of Fv-PrP, Fv-PrPN1, and actin in primary hippocampal neurons isolated from transgenic mice expressing murine Fv-PrP. PrPN1 was immunoprecipitated from the culture medium. Cell lysates were treated with PNGase before Fv-PrP detection. Western blots are representative of at least three independent experiments.

Antibody-mediated PrP^C cross-linking also results in the rapid production of ROS (Schneider et al., 2003). Similarly, we observed an increased number of fluorescent cells using the ROS-sensitive probe DCF-DA following 30 min incubation with AP20187 (Fig. 2*B*).

PrP^C homodimerization increases PrPC1 and PrPN1 levels in cell lines and primary neurons

The HD is essential for PrP^C homodimerization and α-cleavage (Rambold et al., 2008; Bremer et al., 2010; Oliveira-Martins et al., 2010). We sought to directly test whether PrP^C homodimerization could modulate the α-cleavage. Since Fv is present in the unstructured domain of PrP^C (Fig. 1), we took advantage of the presence of the HA tag in the Fv domain to immunoprecipitate PrPN1 from the culture medium of Fv-PrP-expressing cells after AP20187 treatment (Fig. 3*A*,*B*). Anti-HA antibodies cannot immunoprecipitate PrPN1 from PrP^C-expressing cells. Enforced homodimerization of Fv-PrP-expressing cells induced a large increase of secreted PrPN1. This was mirrored by a significant increase in PrPC1 levels following deglycosylation of cell lysates

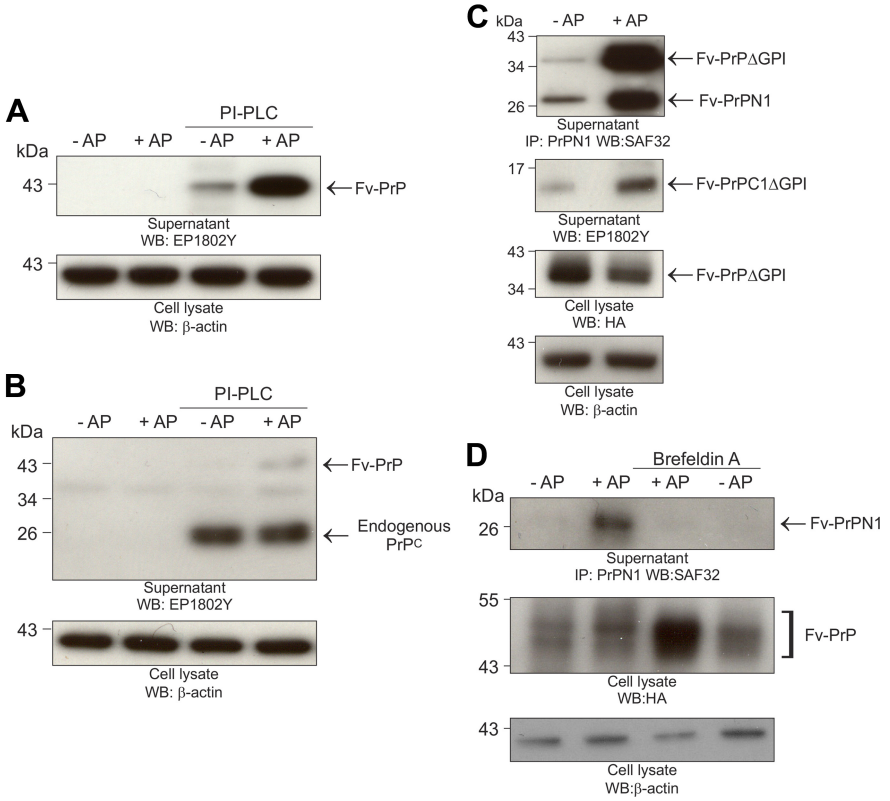

Figure 4. Dimerization of PrP^C increases its trafficking to the cell surface. ***A***, ***B***, Fv-PrP-expressing cells (***A***) and primary hippocampal neurons expressing murine Fv-PrP (***B***) were treated with vehicle (−AP) or AP20187 (+AP) for 4 h. Cells were subsequently washed and treated with PI-PLC. Released Fv-PrP was treated with PNGase F and detected in the medium with EP1802Y antibodies. ***C***, Fv-PrPΔGPI-expressing cells were treated with vehicle (−AP) or AP20187 (+AP) for 20 h. Secreted Fv-PrPΔGPI and PrPN1 were detected with anti-HA antibodies. Fv-PrPC1ΔGPI was detected in the medium with EP1802Y antibodies. ***D***, Fv-PrP-expressing cells were untreated or treated with the fungal metabolite brefeldin A before the addition of AP20187 (+AP) or vehicle (−AP) for 4 h. Fv-PrPN1 and Fv-PrP were quantified in the culture medium and the cell lysate, respectively. All Western blots are representative of three distinct experiments, and equal loading was assessed with anti-actin antibodies.

with PNGase F (Fig. 3*A*,*B*). As expected, AP20187 treatment did not modify PrPC1 levels in PrP^C-expressing cells (Fig. 3*A*). Interestingly, SAF32-mediated cross-linking did not alter PrPN1 and PrPC1 levels (Fig. 3*A*,*B*). This result confirms that homodimerization of PrP^C at the cell surface does not modulate the α-cleavage or that antibodies binding inhibit the α-cleavage probably due to steric hindrance, and validates the use of the inducible dimerization strategy for this study.

To examine the role of PrP^C homodimerization *in vivo*, we created a transgenic mouse line expressing murine Fv-PrP (MoFv-PrP) in PrP^C genomic context on a wild-type C57BL/6 background (Borchelt et al., 1996). Homodimerization of PrP^C in primary hippocampal neurons isolated from E15 homozygote transgenic mice (MoFv-PrP$^{+/+}$) resulted in a large increase of PrPN1 in the supernatant, confirming our previous results in cultured cells (Fig. 3*C*) even though Fv-PrP levels represent only 10% of total PrP levels in these mice (data not shown).

Homodimerization increases PrP^C levels at the cell surface

Since α-cleavage occurs in the secretory pathway (Walmsley et al., 2009), the increase in PrPN1 and PrPC1 levels may result from either an increase of PrP^C secretion or an activation of α-cleavage. To determine whether PrP^C homodimerization increases PrP^C secretion, Fv-PrP-expressing cells were treated with vehicle or AP20187. After 4 h, cells were washed and treated with PI-PLC to release GPI-anchored Fv-PrP from the cell surface, and proteins released in the cell supernatant were deglycosylated to better compare PrP^C levels. Western blot analysis shows that PrP^C levels are clearly enhanced postdimerization (Fig. 4*A*). We confirmed that homodimerization increases cell surface PrP^C in primary hippocampal neurons isolated from MoFv-PrP$^{+/+}$ transgenic mice (Fig. 4*B*). Importantly, actin loading controls confirmed that similar amounts of cells were used in these experiments.

We reasoned that, if PrP^C homodimerization enhances its trafficking to the plasma membrane, homodimerization of PrPΔGPI, a mutant without a GPI anchor and constitutively secreted outside of the cells, should result in a large increase of PrPΔGPI levels in the culture medium. To test this proposition, we generated a stable HEK293 cell line expressing Fv-PrPΔGPI. Similar to Fv-PrP, Fv-PrPΔGPI-expressing cells treated with AP20187 produced higher levels of PrPN1 and PrPC1ΔGPI compared with untreated cells (Fig. 4*C*). This result also confirms that α-cleavage is independent of the GPI anchor (Walmsley et al., 2009), thus indicating that homodimerization-induced cleavage of PrP^C has the same characteristics as normal α-cleavage. More interestingly, in agreement with our hypothesis, we noticed that levels of secreted Fv-PrPΔGPI were also considerably enhanced.

Since enhanced trafficking results in increased production of α-cleavage catabolites, interfering with PrP^C trafficking to the cell surface should inhibit homodimerization-induced increase in PrPN1. To test this assumption, Fv-PrP-expressing cells were treated with the fungal metabolite brefeldin A before the addition of AP20187. Brefeldin A inhibits the transport of proteins from the ER to the Golgi (Lippincott-Schwartz et al., 1989). As expected, brefeldin A completely prevented the increase of PrPN1 levels in AP20187-treated cells (Fig. 4*D*).

Overall, our results establish that dimerization facilitates PrP^C trafficking through the secretory pathway to the plasma membrane and largely increases the production of PrPN1 and PrPC1.

Dimerization-mediated α-cleavage of PrP^C is independent of ADAM8, 10, and 17

The two metalloproteases ADAM10 and ADAM17 were initially proposed to be the proteases that are responsible for constitutive and PKC-regulated α-cleavage of PrP^C, respectively, yet their involvement is currently a matter of debate (Vincent et al., 2001; Taylor et al., 2009; Oliveira-Martins et al., 2010; Altmeppen et al., 2011). Recent results suggest that ADAM8 regulates PrP^C α-cleavage in skeletal muscle (Liang et al., 2012). In addition, although ADAMs are mostly present at the plasma membrane and PrP^C α-cleavage occurs in the late secretory pathway (Walmsley et al., 2009), there is some evidence that ADAMs can also process different substrate in the late secretory pathway (Horiuchi et al., 2007; Groma et al., 2011). Overall, the possible role of ADAMs in the increase of PrPN1 levels after PrP^C dimerization is

a hypothesis that could not be ignored. To address the role of ADAM8, 10, and 17 in dimerization-induced α-cleavage of PrP^C, we first determined their expression. Total cellular RNA was extracted, and RT-PCR was performed using specific primers targeting each ADAM. Only ADAM10 and ADAM17 were expressed in our cultured cells, ruling out any function for ADAM8 (Fig. 5*A*). Amplification of ADAM8 was verified in the human monocytic cell line U-937 (Yoshida et al., 1990). To assess the role of ADAM10 and ADAM17, we used the metalloproteinase inhibitor marimastat. Marimastat did not prevent the large secretion of PrPN1 after PrP^C dimerization (Fig. 5*B*). Efficacy of marimastat was verified with the normal processing of the N-cadherin by ADAM10, which produces a fragment termed CTF (Reiss et al., 2005). In our experimental conditions, marimastat efficiently inhibited the accumulation of CTF (Fig. 5*B*). Although this pharmacological approach indicates that ADAM10 and 17 are unlikely to be involved in PrPN1 production after AP20187 treatment of Fv-PrP-expressing cells, the role of constitutively active ADAM10 and PKC-regulated ADAM17 was addressed in a follow-up experiment. Indeed, SAF32 antibody-mediated dimerization of PrP^C leads to PKC activation, p44^{ERK1} and p42^{ERK2} phosphorylation, and ROS production (Schneider et al., 2003). Similarly, we showed in Figure 2 that AP20187-induced PrP^C dimerization also induces p44^{ERK1} and p42^{ERK2} phosphorylation, and ROS production, suggesting that PKC may be activated after AP20187-mediated dimerization, leading to ADAM17 activation. We transfected HEK293 cells stably expressing Fv-PrP with ADAM10 or ADAM17 siRNAs. siRNAs targeting ADAM10 and ADAM17 led to an important reduction of the corresponding proteins compared with control cells or cells treated with the unrelated siRNAs targeting the lamin A/C (Fig. 5*C*). Reduction of ADAM10 or ADAM17 expression did not result in a significant decrease of PrPN1 recovered in the supernatant after dimerization of Fv-PrP (Fig. 5*C*). Together, our results confirm that neither ADAM10 nor ADAM17 is implicated in the α-cleavage of PrP^C.

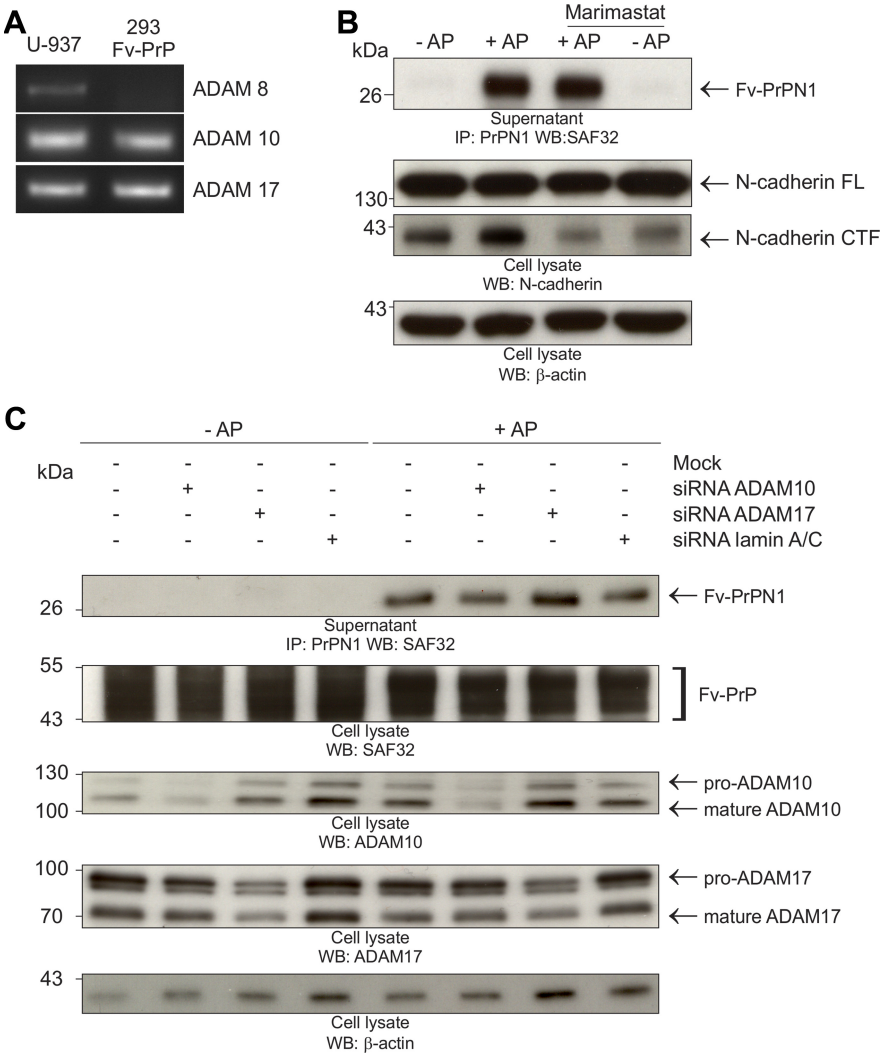

Figure 5. ADAM8, ADAM10, and ADAM17 metalloproteases are not the α-PrPases. ***A***, ADAM8, 10, and 17 mRNA expression in human monocytic cells U-937 and Fv-PrP-expressing cells were assessed by standard RT-PCR. ***B***, Western blot analysis of PrPN1, N-cadherin FL, N-cadherin CTF, and actin with anti-HA, anti-cadherin, and anti-actin antibodies. Fv-PrP-expressing cells were treated with AP20187 (+AP) or vehicle (−AP) in the absence or presence of the general metalloprotease inhibitor marimastat. PrPN1 was immunoprecipitated from the culture medium. Efficiency of marismastat was confirmed with the proteolysis of the N-cadherin detected with an anti-N-cadherin targeting the C-terminal domain of the N-cadherin (CTF) from the cell lysate. ***C***, Pooled siRNAs targeting ADAM10 or ADAM17 or the unrelated lamin A/C and mock treatment were delivered twice to Fv-PrP-expressing cells before dimerization. Fv-PrPN1 was quantified from the culture medium. ADAM10 and ADAM17 knockdown was confirmed from the cell lysate with an anti-ADAM10 or anti-ADAM17 antibodies. All Western blots are representative of three distinct experiments.

PrP^C homodimerization protects cells against Aβ oligomers toxicity

PrP^C mediates toxic signaling of β-sheet-rich oligomers via its N-terminal domain, and a secreted version of PrP^C N-terminal domain significantly interfered with toxic signaling (Resenberger et al., 2011). Similarly, we reasoned that enforced homodimerization of PrP^C and subsequent increase of secreted PrPN1 may also interfere with β-sheet-rich oligomers toxicity. To test this hypothesis, PrP^C-expressing cells grown on coverslips were transferred into cell culture dishes with CHO-7PA2 cells excreting toxic Aβ oligomers (Podlisny et al., 1995; Walsh et al., 2002). The medium was changed with either conditioned medium from Fv-PrP cells treated with AP20187 (+PrPN1) or medium from Fv-PrP cells treated with vehicle (−PrPN1). The presence of monomeric and SDS-stable oligomeric species was detected in conditioned medium from CHO-7PA2 cells (Fig. 6*A*). Aβ oligomer-mediated apoptotic cell death was determined by activated caspase-3 (Fig. 6*B*). Remarkably, conditioned medium from Fv-PrP cells treated with AP20187 significantly reduced apoptotic cell death activation of caspase-3 by 71% (Fig. 6*B*, inset). We also determined the cytoxicity of Aβ oligomers and the protective effect from PrPN1 secreted by Fv-PrP-expressing cells treated with AP20187 (+PrPN1) with TUNEL assays. Similarly, conditioned medium from Fv-PrP cells treated with AP20187

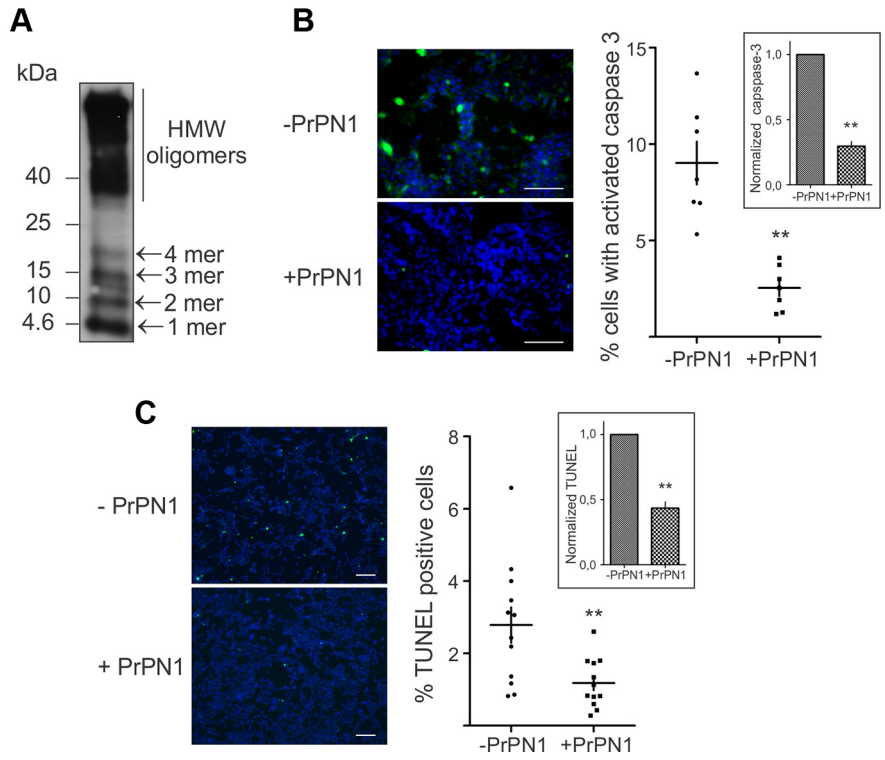

Figure 6. Neuroprotection activity of PrPN1. ***A***, Western blot of conditioned medium from CHO-7PA2 cells excreting Aβ oligomers with monoclonal 6E10 antibodies. ***B***, ***C***, PrP^C-expressing cells growing on coverslips were cocultured with Aβ-secreting CHO-7PA2 cells in the presence of conditioned medium from AP20187-treated (+PrPN1) or vehicle-treated (−PrPN1) Fv-PrP cells. PrP^C-expressing cells were collected after 48 h of coculture, and apoptotic cell death was quantified by immunofluorescence against active caspase-3 (***B***), and TUNEL assays (***C***) as described in Materials and Methods (*$p < 0.05$; **$p < 0.005$). The insets show the percentage of active caspase-3 (***B***)- or TUNEL (***C***)-positive cells in the presence of conditioned medium from AP20187-treated Fv-PrP cells (+PrPN1), compared with vehicle-treated Fv-PrP cells (−PrPN1). Scale bar, 100 μm. Error bars indicate SEM.

significantly reduced the number of cells positive for TUNEL staining by 56% (Fig. 6*C*, inset).

Discussion

α-Cleavage and generation of the GPI-anchored C-terminal PrPC1 fragment and the secreted N-terminal PrPN1 fragment is a typical posttranslational modification of PrP^C. The importance of the α-cleavage is illustrated by increasing evidence that both PrPN1 and PrPC1 represent potential therapeutic molecules for the treatment of prion diseases (Westergard et al., 2011; Guillot-Sestier et al., 2012). In this study, we show that PrP^C homodimerization increases its trafficking to the plasma membrane, and we identify homodimerization as an important mechanism in the control of PrPC1 and PrPN1 levels.

Although we used an artificial strategy to enforce the dimerization of PrP^C, we believe that our results are highly relevant to *in vivo* conditions. A growing number of studies have highlighted the importance of dimerization in the biology of the prion protein. PrP^C forms dimers in bovine and mouse brain homogenates, and in neuroblastoma cells (Priola et al., 1995; Meyer et al., 2000; Rambold et al., 2008). The formation of such dimers is directly linked to the stress-protective activity of PrP^C in cells, and prion-infected cells, which are impaired in PrP^C dimerization, are hypersensitive to stress conditions (Rambold et al., 2008). In contrast, the dimerization between PrP^C and its pathogenic conformer PrP^{Sc} is a key step in the propagation of PrP^{Sc} (Prusiner et al., 1990). Thus, PrP^C dimerization is an important mechanism in normal and pathological conditions.

Several studies point to PrP^C as a plasma membrane receptor able to activate a variety of intracellular signaling pathways (Linden et al., 2008; Schneider et al., 2011). In particular, antibody-mediated dimerization of PrP^C at the plasma membrane induces the cell survival ERK cascade and the production of ROS (Schneider et al., 2003; Monnet et al., 2004; Rambold et al., 2008). AP20187-mediated PrP^C homodimerization also resulted in the transient activation of ERK. This activation was much more robust with antibodies against PrP^C, but it was consistently observed in our experiments. The production of ROS after AP20187 treatment was also clearly evident.

In contrast to PrP^C dimerization at the plasma membrane with antibodies, enforced dimerization using cell-permeable AP20187 revealed an unexpected finding, a dramatic increase in secreted PrPN1. The large increase in PrPN1 levels on top of dimerization-induced signaling adds an additional level to the neuroprotective activity of PrP^C. Thus, we propose that dimerization-dependent neuroprotective activity of PrP^C occurs as a two-step mechanism. First, dimerization at the plasma membrane triggers prosurvival intracellular signaling cascades. Second, intracellular dimerization increases both neuroprotective PrPN1 and dominant-negative inhibitor of PrP^{Sc} formation PrPC1. In addition, since the levels of cell surface PrP^C increase following intracellular dimerization, there is more protein available at the plasma membrane to interact with a putative neuroprotective ligand. Overall, homodimerization provides PrP^C with an extremely efficient neuroprotective activity.

PrP^{Sc} binding to plasma membrane PrP^C corrupts PrP^C protective activity (Rambold et al., 2008). Binding of other β-sheet-rich molecules to PrP^C at the cell surface, including Aβ oligomers also induces PrP^C-mediated toxic signaling (Resenberger et al., 2011). The increase of PrP^C at the cell surface following its dimerization may facilitate the toxic activity of β-sheet-rich oligomers. However, the parallel increase in PrPN1 might prevent the corruption of PrP^C by β-sheet-rich oligomers. This is supported by the observation that PrPN1 antagonizes β-sheet-rich oligomers toxic signaling (Guillot-Sestier et al., 2009, 2012; Resenberger et al., 2011) (Fig. 6).

Many aspects of the α-cleavage are still elusive, including the identity of the α-PrPases and the limited sequence specificity. More evidence is now challenging the implication of ADAM10 and ADAM17 as the principal α-PrPases (Vincent et al., 2001; Laffont-Proust et al., 2005; Taylor et al., 2009; Altmeppen et al., 2011). Taylor et al. clearly demonstrated that the α-cleavage of PrP^C was not affected by the absence of both ADAM10 and ADAM17 *in cellulo* (Taylor et al., 2009). In addition, ADAM10-deficient mice have no alteration in levels of PrPC1 (Altmeppen et al., 2011). Here, we showed that inhibition of ADAM10 and ADAM17 by the general metalloprotease inhibitor marimastat and knockdown of both ADAM10 and ADAM17 expression did

not affect the release of PrPN1 in the culture medium under dimerization conditions.

Our observation that dimerization facilitates PrP^C trafficking to the plasma membrane is reminiscent of other cell receptors, including G-protein-coupled receptors (GPCRs) (Terrillon and Bouvier, 2004). For some GPCRs, it is well established that dimerization leads to adequate folding, which is mandatory to escape the endoplasmic reticulum and continue the progression toward the cell surface. Proper folding of PrP^C is a major issue for the biology of this protein in health and diseases, and the impact of dimerization as a possible avenue to increase the efficiency of PrP^C folding and trafficking deserves further investigations.

References

Altmeppen HC, Prox J, Puig B, Kluth MA, Bernreuther C, Thurm D, Jorissen E, Petrowitz B, Bartsch U, De Strooper B, Saftig P, Glatzel M (2011) Lack of a-disintegrin-and-metalloproteinase ADAM10 leads to intracellular accumulation and loss of shedding of the cellular prion protein in vivo. Mol Neurodegener 6:36.

Borchelt DR, Davis J, Fischer M, Lee MK, Slunt HH, Ratovitsky T, Regard J, Copeland NG, Jenkins NA, Sisodia SS, Price DL (1996) A vector for expressing foreign genes in the brains and hearts of transgenic mice. Genet Anal 13:159–163.

Brandner S, Isenmann S, Raeber A, Fischer M, Sailer A, Kobayashi Y, Marino S, Weissmann C, Aguzzi A (1996) Normal host prion protein necessary for scrapie-induced neurotoxicity. Nature 379:339–343.

Bremer J, Baumann F, Tiberi C, Wessig C, Fischer H, Schwarz P, Steele AD, Toyka KV, Nave KA, Weis J, Aguzzi A (2010) Axonal prion protein is required for peripheral myelin maintenance. Nat Neurosci 13:310–318.

Büeler H, Aguzzi A, Sailer A, Greiner RA, Autenried P, Aguet M, Weissmann C (1993) Mice devoid of PrP are resistant to scrapie. Cell 73:1339–1347.

Chen SG, Teplow DB, Parchi P, Teller JK, Gambetti P, Autilio-Gambetti L (1995) Truncated forms of the human prion protein in normal brain and in prion diseases. J Biol Chem 270:19173–19180.

Eggert S, Midthune B, Cottrell B, Koo EH (2009) Induced dimerization of the amyloid precursor protein leads to decreased amyloid-beta protein production. J Biol Chem 284:28943–28952.

Goggin K, Bissonnette C, Grenier C, Volkov L, Roucou X (2007) Aggregation of cellular prion protein is initiated by proximity-induced dimerization. J Neurochem 102:1195–1205.

Groma G, Grskovic I, Schael S, Ehlen HW, Wagener R, Fosang A, Aszodi A, Paulsson M, Brachvogel B, Zaucke F (2011) Matrilin-4 is processed by ADAMTS-5 in late Golgi vesicles present in growth plate chondrocytes of defined differentiation state. Matrix Biol 30:275–280.

Guillot-Sestier MV, Sunyach C, Druon C, Scarzello S, Checler F (2009) The alpha-secretase-derived N-terminal product of cellular prion, N1, displays neuroprotective function in vitro and in vivo. J Biol Chem 284:35973–35986.

Guillot-Sestier MV, Sunyach C, Ferreira ST, Marzolo MP, Bauer C, Thevenet A, Checler F (2012) Alpha-secretase-derived fragment of cellular prion, N1, protects against monomeric and oligomeric amyloid beta (abeta)-associated cell death. J Biol Chem 287:5021–5032.

Horiuchi K, Le Gall S, Schulte M, Yamaguchi T, Reiss K, Murphy G, Toyama Y, Hartmann D, Saftig P, Blobel CP (2007) Substrate selectivity of epidermal growth factor-receptor ligand sheddases and their regulation by phorbol esters and calcium influx. Mol Biol Cell 18:176–188.

Kwak HI, Mendoza EA, Bayless KJ (2009) ADAM17 co-purifies with TIMP-3 and modulates endothelial invasion responses in three-dimensional collagen matrices. Matrix Biol 28:470–479.

Laffont-Proust I, Faucheux BA, Hässig R, Sazdovitch V, Simon S, Grassi J, Hauw JJ, Moya KL, Haïk S (2005) The N-terminal cleavage of cellular prion protein in the human brain. FEBS Lett 579:6333–6337.

Lewis V, Hill AF, Haigh CL, Klug GM, Masters CL, Lawson VA, Collins SJ (2009) Increased proportions of C1 truncated prion protein protect against cellular M1000 prion infection. J Neuropathol Exp Neurol 68:1125–1135.

Liang J, Wang W, Sorensen D, Medina S, Ilchenko S, Kiselar J, Surewicz WK, Booth SA, Kong Q (2012) Cellular prion protein regulates its own alpha-cleavage through ADAM8 in skeletal muscle. J Biol Chem 287:16510–16520.

Linden R, Martins VR, Prado MA, Cammarota M, Izquierdo I, Brentani RR (2008) Physiology of the prion protein. Physiol Rev 88:673–728.

Lippincott-Schwartz J, Yuan LC, Bonifacino JS, Klausner RD (1989) Rapid redistribution of Golgi proteins into the ER in cells treated with brefeldin A: evidence for membrane cycling from Golgi to ER. Cell 56:801–813.

Lopes MH, Hajj GN, Muras AG, Mancini GL, Castro RM, Ribeiro KC, Brentani RR, Linden R, Martins VR (2005) Interaction of cellular prion and stress-inducible protein 1 promotes neuritogenesis and neuroprotection by distinct signaling pathways. J Neurosci 25:11330–11339.

Mallucci G, Dickinson A, Linehan J, Klöhn PC, Brandner S, Collinge J (2003) Depleting neuronal PrP in prion infection prevents disease and reverses spongiosis. Science 302:871–874.

Mangé A, Béranger F, Peoc'h K, Onodera T, Frobert Y, Lehmann S (2004) Alpha- and beta- cleavages of the amino-terminus of the cellular prion protein. Biol Cell 96:125–132.

Meyer RK, Lustig A, Oesch B, Fatzer R, Zurbriggen A, Vandevelde M (2000) A monomer-dimer equilibrium of a cellular prion protein (PrPC) not observed with recombinant PrP. J Biol Chem 275:38081–38087.

Monnet C, Gavard J, Mège RM, Sobel A (2004) Clustering of cellular prion protein induces ERK1/2 and stathmin phosphorylation in GT1-7 neuronal cells. FEBS Lett 576:114–118.

Oliveira-Martins JB, Yusa S, Calella AM, Bridel C, Baumann F, Dametto P, Aguzzi A (2010) Unexpected tolerance of alpha-cleavage of the prion protein to sequence variations. PLoS One 5:e9107.

Podlisny MB, Ostaszewski BL, Squazzo SL, Koo EH, Rydell RE, Teplow DB, Selkoe DJ (1995) Aggregation of secreted amyloid beta-protein into SDS-stable oligomers in cell culture. J Biol Chem 270:9564–9570.

Priola SA, Caughey B, Wehrly K, Chesebro B (1995) A 60-kDa prion protein (PrP) with properties of both the normal and scrapie-associated forms of PrP. J Biol Chem 270:3299–3305.

Prusiner SB, Scott M, Foster D, Pan KM, Groth D, Mirenda C, Torchia M, Yang SL, Serban D, Carlson GA (1990) Transgenetic studies implicate interactions between homologous PrP isoforms in scrapie prion replication. Cell 63:673–686.

Prusiner SB, Scott MR, DeArmond SJ, Cohen FE (1998) Prion protein biology. Cell 93:337–348.

Rambold AS, Müller V, Ron U, Ben-Tal N, Winklhofer KF, Tatzelt J (2008) Stress-protective signalling of prion protein is corrupted by scrapie prions. EMBO J 27:1974–1984.

Reiss K, Maretzky T, Ludwig A, Tousseyn T, de Strooper B, Hartmann D, Saftig P (2005) ADAM10 cleavage of N-cadherin and regulation of cell-cell adhesion and beta-catenin nuclear signalling. EMBO J 24:742–752.

Resenberger UK, Harmeier A, Woerner AC, Goodman JL, Müller V, Krishnan R, Vabulas RM, Kretzschmar HA, Lindquist S, Hartl FU, Multhaup G, Winklhofer KF, Tatzelt J (2011) The cellular prion protein mediates neurotoxic signalling of beta-sheet-rich conformers independent of prion replication. EMBO J 30:2057–2070.

Roucou X, Gains M, LeBlanc AC (2004) Neuroprotective functions of prion protein. J Neurosci Res 75:153–161.

Schneider B, Mutel V, Pietri M, Ermonval M, Mouillet-Richard S, Kellermann O (2003) NADPH oxidase and extracellular regulated kinases 1/2 are targets of prion protein signaling in neuronal and nonneuronal cells. Proc Natl Acad Sci U S A 100:13326–13331.

Schneider B, Pietri M, Pradines E, Loubet D, Launay JM, Kellermann O, Mouillet-Richard S (2011) Understanding the neurospecificity of prion protein signaling. Front Biosci 16:169–186.

Spencer DM, Wandless TJ, Schreiber SL, Crabtree GR (1993) Controlling signal transduction with synthetic ligands. Science 262:1019–1024.

Steele AD, Lindquist S, Aguzzi A (2007) The prion protein knockout mouse: a phenotype under challenge. Prion 1:83–93.

Sunyach C, Cisse MA, da Costa CA, Vincent B, Checler F (2007) The C-terminal products of cellular prion protein processing, C1 and C2, exert distinct influence on p53-dependent staurosporine-induced caspase-3 activation. J Biol Chem 282:1956–1963.

Taylor DR, Parkin ET, Cocklin SL, Ault JR, Ashcroft AE, Turner AJ, Hooper NM (2009) Role of ADAMs in the ectodomain shedding and conformational conversion of the prion protein. J Biol Chem 284:22590–22600.

Terrillon S, Bouvier M (2004) Roles of G-protein-coupled receptor dimerization. EMBO Rep 5:30–34.

Vincent B, Paitel E, Saftig P, Frobert Y, Hartmann D, De Strooper B, Grassi J, Lopez-Perez E, Checler F (2001) The disintegrins ADAM10 and TACE contribute to the constitutive and phorbol ester-regulated normal cleavage of the cellular prion protein. J Biol Chem 276: 37743–37746.

Walmsley AR, Watt NT, Taylor DR, Perera WS, Hooper NM (2009) Alpha-cleavage of the prion protein occurs in a late compartment of the secretory pathway and is independent of lipid rafts. Mol Cell Neurosci 40:242–248.

Walsh DM, Klyubin I, Fadeeva JV, Cullen WK, Anwyl R, Wolfe MS, Rowan MJ, Selkoe DJ (2002) Naturally secreted oligomers of amyloid beta protein potently inhibit hippocampal long-term potentiation in vivo. Nature 416:535–539.

Wessel D, Flügge UI (1984) A method for the quantitative recovery of protein in dilute solution in the presence of detergents and lipids. Anal Biochem 138:141–143.

Westergard L, Turnbaugh JA, Harris DA (2011) A naturally occurring C-terminal fragment of the prion protein (PrP) delays disease and acts as a dominant-negative inhibitor of PrPSc formation. J Biol Chem 286:44234–44242.

Yoshida S, Setoguchi M, Higuchi Y, Akizuki S, Yamamoto S (1990) Molecular cloning of cDNA encoding MS2 antigen, a novel cell surface antigen strongly expressed in murine monocytic lineage. Int Immunol 2:585–591.